An experimental study of the crater evolution by impact of a drop onto a shallow pool

N.P. van Hinsberg*, I.V. Roisman, C. Tropea
Chair of Fluid Mechanics and Aerodynamics
Technische Universitaet Darmstadt
Darmstadt, Germany

The evolution of a crater produced by impact of a drop onto a shallow pool of the same liquid is studied experimentally. The crater contour is observed by high-resolution imaging. The time evolution of various parameters, like the crater depth and crater diameter, are reported as a function of the shallow pool depth, the drop impact velocity and the liquid properties. The results indicate that the depth evolution is independent of the drop impact velocity and liquid properties, whereas for the diameter of the crater a clear influence of each parameter is seen.

Introduction

Spray impact and drop impact onto a liquid film have great relevance in many technical applications, such as surface cooling, spray injection in internal combustion engines and painting. Droplet surface interaction is also important in agriculture, atmospheric sciences such as thunderstorm electrification [1] and natural phenomena such as waterfall electrification [2]. Also it is responsible for the corrosion of turbine blades.

The sequence of events which occurs during the impact of single drops onto films or pools of various depths have been described by many authors [3]. Much research has been conducted to understand the evolution of the maximum crater depth in relation to the crown formation, splashing, the Worthington jet height and bubble entrainment during single drop impact. Less attention, however, has been paid to the phenomena taking place below the surface, in particular the evolution of the impact crater in shallow pools ([4], [5], [6]), which is important for spray cooling.

Specific objectives

The specific objective of the present study is to understand the phenomena occuring during the impact of a single drop onto a shallow pool of the same liquid, by changing various input parameters, like the liquid properties, the pool depth and the drop impact velocity. A particular aspect of interest in the present discussion is the evolution of the crater formed after impact, primarily the expansion and the contraction phases.

Experimental arrangement

A schematic of the experimental setup is shown in Figure 1. Drops are generated using a medical syringe pump which is programmed to dispense the liquid at a constant flow rate of about 0.40 μl/s - 1.81 μl/s depending on the fluid used. The drop is formed and grows at the tip of the needle until its weight exceeds the net upward surface tension force on the drop and the drop detaches from the needle. The rate at which drops grow and fall can be changed by adjusting the speed of the stepping motor of the syringe pump. The falling drops are enclosed in a vertical 32 mm Plexiglass tube to protect them from air flow disturbances. The drops pass a light barrier before falling into the center of a Perspex cylinder of 90 mm diameter used to hold the target liquid. The impact event is completed in a small fraction of the time required for the surface waves to propagate to the edge of the cylinder, as its diameter about 31 to 42 times larger than the drop diameter. Therefore the cylinder is large enough to avoid interference of the wave reflections from the sides with the impact process. An adequate time is allowed to elapse between subsequent impacts to assure a still surface of

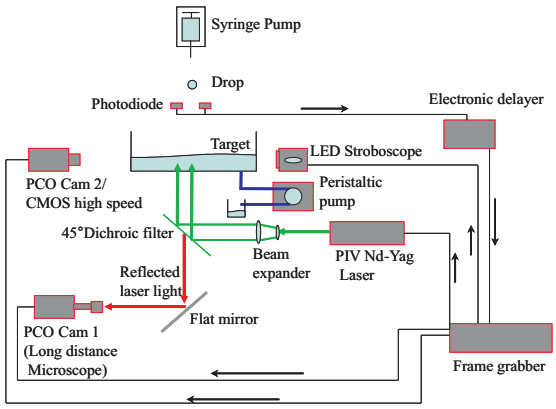

Figure 1: Experimental setup for crater evolution and velocity measurements

* Corresponding author:
n.van.hinsberg@sla.tu-darmstadt.de
Associated Web site: www.sla.tu-darmstadt.de
Proceedings of the 21^{th} ILASS - Europe Meeting 2007

Table 1: Physical properties of the liquids used and the range of investigated parameters

	$20°C$					
	Density (kg/m^3)	Viscosity (Ns/m^2)	Surface tension Coeff (N/m)	Ohnesorge number	Weber number	Capillary number
Distilled Water	999	$9.9{\cdot}10^{-4}$	$7.27{\cdot}10^{-2}$	0.0021	137 - 312	0.022 - 0.039
1-Propanol	805	$2.3{\cdot}10^{-3}$	$2.36{\cdot}10^{-2}$	0.0112	204 - 644	0.154 - 0.301

the target liquid before impact. The fluid of the drops and in the liquid are the same for each experiment. The light barrier activates an electronic delay circuit that triggers the imaging system, consisting of two PCO Sensicam CCD cameras, one backlit by a stroboscope and the other by a PIV Nd:YAG-laser. The first camera (Cam 1, Figure 1) looks at the free surface of the target liquid and is used together with an Nd:YAG PIV laser. This camera is equipped with an extended 105 mm Nikkor Nikon lens working as a long distance microscope, positioned horizontally, aligned with the free surface through a 45° flat mirror, and used for recording the exact impact instant. The other camera (Cam 2) is fitted with an extended 50 mm Cosmicar Television Lens for a good balance between the required spatial resolution and the necessary field of view. This camera is back-lit using a StroboLED stroboscope at a pulse time of 10 μs together with a glass diffuser to produce a uniform, bright, diffused light source. The observations are performed using a multiple exposure technique based on the high repeatability of the impact process.

For single drop impact three parameters are of importance: the Ohnesorge number and Weber number, the former defined as $Oh = \mu/(\sigma\rho D_p)^{0.5}$, the latter as $We = \rho U^2 D_p/\sigma$, and the dimensionless pool depth $H^* = H/D_p$. Here μ, σ and ρ are, respectively, the dynamic viscosity, surface tension and density of the tested liquids, D_p the drop diameter, U the drop velocity before impact and H the film thickness or pool depth.

To investigate the influence of the liquid properties on the crater evolution, the results for distilled water and 1-Propanol are compared.
The initial drop diameter is fixed at 2.97 ± 0.11 mm for distilled water and 2.22 ± 0.05 mm for 1-Propanol. Varying the impact height between 150 mm and 450 mm leads to a variation of the drop impact velocity. The drop velocity just before impact is calculated from a distance measurement and a pre-set time delay between two subsequent exposures. The impact velocity is 1.68 ± 0.096 m/s to 2.91 ± 0.193 m/s for distilled water and 1.7 ± 0.140 m/s to 2.83 ± 0.085 m/s for 1-Propanol, resulting in corresponding Weber numbers in the range of 137 to 312 and 204 to 644.

The depth of the pool is varied from 1.5 mm to 6.0 mm for both fluids. This leads to a change in dimensionless film thickness from $H^* = 0.68$ to $H^* = 2.7$ for 1-Propanol and $H^* = 0.50$ to $H^* = 2.0$ for distilled water. These values of H^* are typical for the case of spray impact. A peristaltic pump with variable flow rate is used to keep the pool depth at constant height, resulting in an error in depth of 3% to 7% for distilled water and 2% to 10% for 1-Propanol. The most important material and impact parameters are given in Table 1.

Results and discussion

The main objective of the present investigation is to understand the phenomena occuring during the impact of a single drop onto a shallow pool,

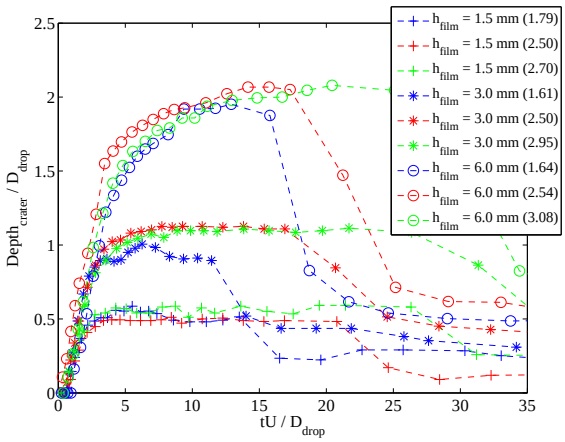

Figure 2: Cavity depth against dimensionless time for distilled water (The numbers in brackets are the drop impact velocities in m/s)

pictures of the event, taken from the side and below the target at different instants after drop impact. Figure 3 shows pictures of the crater from the side at three different time instants during crater collapse. A clear capillary wave is seen travelling down along the crater wall, during which the shape of the crater changes from hemispherical (a) to conical (c).
The evolution of the main parameters is described below. The depth is analysed by measuring the lowest point of the crater, whereas the diameter of the crater is measured at four different depth locations inside the film, as defined in Figure 3.
The analysis is split up into three main parts, i.e. the influence of the impact velocity, the pool depth

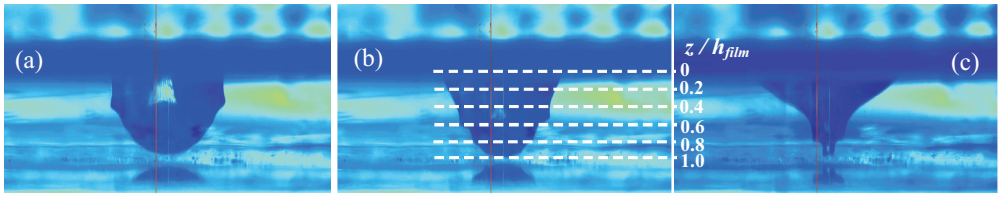

Figure 3: Shape of the crater produced by drop impact at various instants of time for 1-Propanol (U = 2.75 m/s; h_{pool} = 6 mm) at tU/D = 28.4 (a), tU/D = 33.4 (b) and tU/D = 39.7 (c)

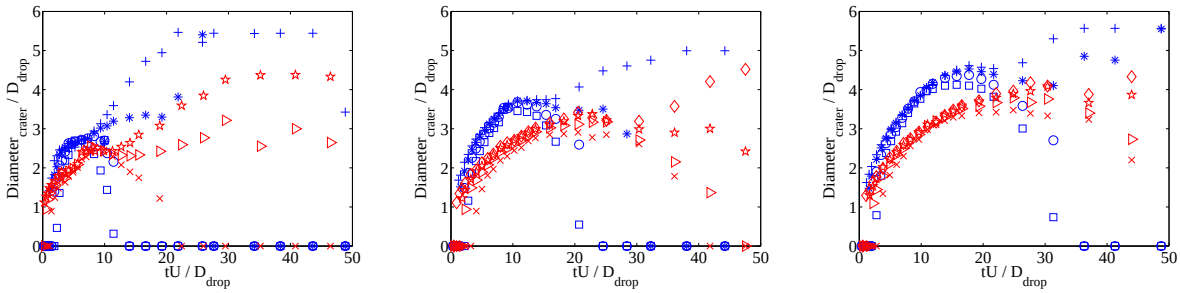

(a) U = 1.58 m/s (b) U = 2.41 m/s (c) U = 2.93 m/s

Figure 4: Influence of drop impact velocity and liquid used on crater evolution for h_{pool} = 3 mm (Water: + z/h_{pool} = 0.20, ∗ z/h_{pool} = 0.40, ∘ z/h_{pool} = 0.60, □ z/h_{pool} = 0.80; 1-Propanol: ◊ z/h_{pool} = 0.20, ★ z/h_{pool} = 0.40, ▷ z/h_{pool} = 0.60, × z/h_{pool} = 0.80)

and the liquid properties on the crater evolution. The time is made dimensionless by velocity times drop diameter, the crater depth and diameter by the drop diameter. For all graphs,we have set t/UD = 0 as the time at which the drop reaches the pool surface.

Influence of drop impact velocity on crater evolution

In Figure 2 the change of the cavity depth with time is given for distilled water for the three investigated pool depths and impact velocities. In general we notice a steep increase in depth in the first time instants, which becomes weaker as the crater nears the bottom of the pool. The slope of the curves for constant pool depth are the same for each velocity. As the crater touches the bottom, the curves level off and the crater stays in contact with the bottom until it collapses and inverses its direction, resulting in a decrease of the crater depth. It is noted that a change in impact velocity, for constant pool depth, has little to no effect on the growth of the crater in depth until the moment the crater has collapsed, and on the time to reach maximum depth. The only effect of the impact velocity on the crater depth is the moment at which the crater starts to retract from the bottom. For lower drop velocities, this moment is sooner and the collapse is faster, but in the end the same minimum depth is reached.

The change of the crater diameter with time is given in Figure 4 for both distilled water and 1-Propanol for the three investigated impact velocities at constant pool depth of 3 mm. The diameter is measured at four different depths inside the pool, i.e. z/h_{pool} = 0.20, 0.40, 0.60 and 0.80 (Figure 3). It can be seen that all curves follow the same trend. In the first time instants a steep growth of the crater diameter is seen, which levels off when the crater nears the bottom of the pool. The steepness with which the diameter increases, decreases for increasing drop impact velocity. As the crater touches the bottom, it cannot grow further in depth, resulting in an increase of the diameter. For larger impact velocities, the maximum diameter is therefore reached at a later time instant and its value is higher. We notice that during the growth period, the values of the diameter for the four depths lie close together, meaning the craters grow with vertical walls.
At some instant, a capillary wave starts moving down along the crater's surface, resulting in a collapse of the crater, as seen in Figure 3. This is seen in Figure 4 as a decrease in diameter at the lower depths in the pool. This decrease starts slow, but accelerates in time. At the same moment, the crater increases in diameter close to the surface of the pool. When the crater has changed to a V-shape, the bottom of the crater reverses its direction upwards (seen in Figure 2 as a decrease of the curves) and a steep increase in diameter is seen for each impact velocity. For all

velocities, the ratio of the time to reach maximum diameter to the time the crater bottom starts moving up is about 2.

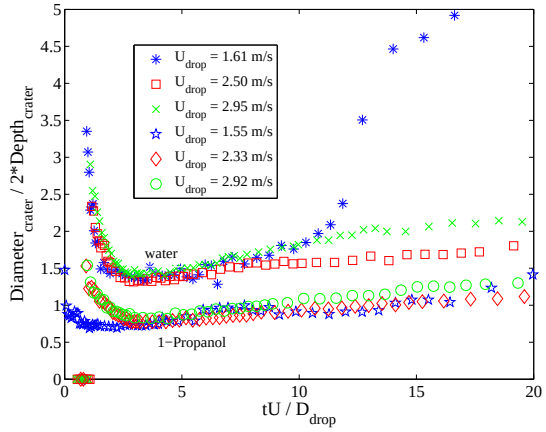

Figure 5: Ratio of the cavity diameter and twice the cavity depth for h_{pool} = 3 mm (Water: $*$ H^* = 0.5, $\square$ H^* = 1, $\times$ H^* = 2; 1-Propanol: $\bigstar$ H^* = 0.5, $\Diamond$ H^* = 1, $\circ$ H^* = 2)

In Figure 5 the ratio of the cavity diameter and twice the cavity depth against time is plotted for both liquids at constant pool depth of 3 mm for U_{drop} = 1.55 to 2.95 m/s. First of all, it is noted that the drop impact velocity has little to no effect on this ratio up to the point where the crater has collapsed, seen as a sharp increase in the diameter to depth ratio for water at U = 1.61 m/s. By increasing the impact velocity, the time to reach the maximum diameter to depth ratio right after collapse is larger as the crater grows longer in diameter. As a result, the collapse of the crater is later, resulting in a delayed steep increase (not shown here, as the start of crater collapse lies beyond tU/D = 20, with the exception of U_{drop} = 1.55 for distilled water).

Influence of pool depth on crater evolution

Three different pool depths have been investigated, 1.5 mm, 3 mm and 6 mm, resulting in dimensionless pool depths of H^* = 0.68 to H^* = 2.7 for 1-Propanol and between H^* = 0.50 and H^* = 2.0 for water.

In Figure 2 the time change of cavity depth is given for distilled water. The increase in depth with time for the crater is the same for all three pool depths at constant drop velocities. The slope has a value of about 0.4 - 0.5. As expected, when the depth of the pool is increased, the crater reaches the bottom of the pool at a later instant.

For every depth and impact velocity, the craters touch the bottom of the pool; the lower the pool depth, the longer the crater stays at the bottom, which is seen as the curves stay horizontally. At constant impact velocity, the instant at which the crater starts to retract is of the same order for different pool depths. The slope of decrease of the crater depth is steeper when the pool depth is larger, as the depth of all craters return at more or less the same level.

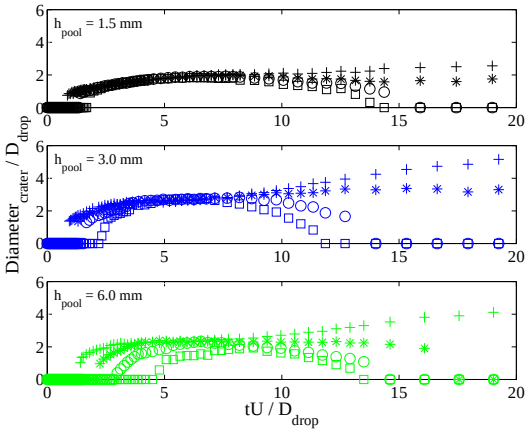

Figure 6: Influence of pool depth on crater diameter evolution in time for distilled water at U = 1.7 m/s ($+$ z/h_{pool} = 0.20, $*$ z/h_{pool} = 0.40, $\circ$ z/h_{pool} = 0.60, $\square$ z/h_{pool} = 0.80)

The change of diameter of the crater for the three different pool depths for distilled water is given in Figure 6 for an impact velocity of U = 1.7 m/s.

Increasing the pool depth leads to a decrease of the steepness of the curves at every depth location (z/h_{pool} = 0.20, 0.40, 0.60 and 0.80). For every impact height, the curves for h_{pool} = 6 mm lie below the curves for h_{pool} = 3 mm, and those lie again below h_{pool} = 1.5 mm; this seen as well in Figure 7, where we notice that during the collapse of the crater the curve for h_{pool} = 3.0 mm lies above the one for h_{pool} = 1.5 mm for both liquids. The difference between the latter two pool depths is smaller than for the first two depths. An exception are the curves for a drop impact velocity of 1.79 m/s and h_{pool} = 1.5 mm, where this curve is much lower as the others. For h_{pool} = 1.5 mm, the values of the diameters at different z/h_{pool} lie on one curve, meaning the crater walls are vertical. For h_{pool} = 3 mm a slight scatter is seen for z/h_{pool} = 0.6 and 0.8, where the diameter increases some instants later, but at the maximum crater diameter before collapse, the walls straighten. For h_{pool} = 6 mm a clear hemispherical crater can be seen, resulting in an increase in diameter one after another for increasing z/h_{pool}. The times at which the maximum crater diameter before collapse is reached is independent of the pool depth.

When doubling the pool depth and keeping the other parameters constant, the ratio of the cavity diameter and twice the cavity depth (Figure 8) will decrease by a factor 2. For all pool depths the

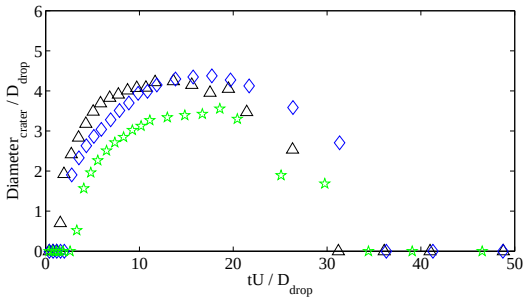

(a) Distilled water; U = 2.91 m/s

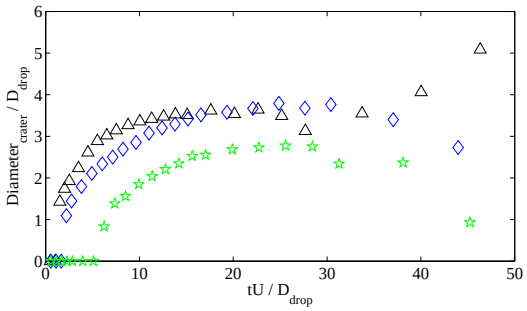

(b) 1-Propanol; U = 2.88 m/s

Figure 7: Influence of pool depth on crater evolution for water and 1-Propanol at z/h_{pool} = 0.6 (△ h_{pool} = 1.5 mm, ◊ h_{pool} = 3.0 mm, ★ h_{pool} = 6.0 mm)

crater is cylindrical right after impact and the slope of the subsequent decrease is the same. For h_{pool} = 1.5 mm, however, this decrease stops sooner as the crater reaches the bottom of the pool, after which the ratio increases sharply before levelling off. During this process, the crater stays cylindrical. As the pool depth increases, it takes longer for the crater to reach the bottom, resulting in a longer decrease of the diameter to depth ratio; in this case the crater gets more hemispherical, i.e. a ratio close to 1. The increase after contact with the pool bottom is lower for h_{pool} = 3 mm and 6 mm, and for h_{pool} = 6 mm the curves stay at a value of 1 until the crater starts to retract upwards. As the craters collapse, the diameter to depth ratios for h_{pool} = 1.5 mm slightly decrease for each velocity, before a sharp increase is seen for each curve as the craters retract upwards.
For h_{pool} = 1.5 mm the maximum diameter to depth ratios before collapse are reached at the instant at which the crater starts to collapse, whereas for h_{pool} = 3 mm and 6 mm they are reached at the same time instant just before the craters retract.

Influence of liquid properties

To investigate the influence of the liquid properties, such as the viscosity and surface tension, on the crater evolution, we have made measurements using distilled water and 1-Propanol, of which the

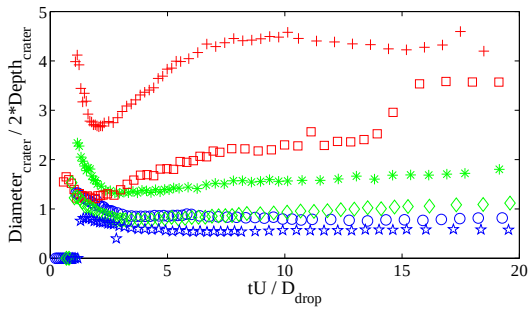

Figure 8: Ratio of the cavity diameter and twice the cavity depth as a function of pool depth for water at U = 2.50 m/s and 1-Propanol at U = 2.36 m/s (Water: + H^* = 0.5, ∗ H^* = 1, ∘ H^* = 2; 1-Propanol: □ H^* = 0.68, ◊ H^* = 1.35, ★ H^* = 2.7)

properties are given in Table 1. For both liquids, we set the same pool depths and drop impact heights, resulting in the same drop velocities just before impact.

In Figure 9 the depth of the crater has been plotted against time for both liquids. In our measurements,

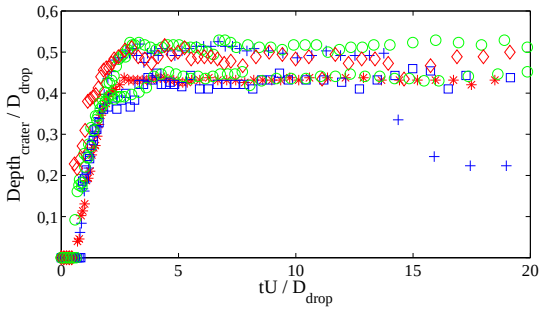

Figure 9: Influence of liquid properties on crater depth evolution in time for H^* = 0.5 (Water: + U = 1.79 m/s, ∗ U = 2.50 m/s, ∘ U = 2.70 m/s; 1-Propanol: □ U = 1.83 m/s, ◊ U = 2.37 m/s, ★ U = 2.83 m/s)

we use the same pool depth, but the drop diameter for 1-Propanol drops is about 25% smaller than for distilled water, resulting in higher values of H^*. To get a good comparison between both liquids, we have divided the measured values of the crater depth for 1-Propanol with the factor $D_{water}/D_{1-Propanol}$ = 1.38 to receive the same H^*-values as for water. We notice that the liquid properties have no influence on the period in which the depth increases up to the moment until maximum depth is reached.
For each pool depth, all curves reach the bottom of the pool at the same time. For 1-Propanol, the decrease in depth after the crater has collapsed starts later, with an increasing time difference for larger pool depths and drop impact heights.

Increasing the pool depth, at constant drop velocity, leads for both liquids to a decrease of the steepness of the curves of the crater diameter, as is seen in Figure 7. It can be seen that the steepness of the curves for distilled water is larger for each pool depth and that the maximum diameter is higher and reached at an earlier time instant. The same behaviour is noted for constant pool depth and increasing drop velocities, as seen in Figure 4.
The collapse of the crater and the accompanying decrease in diameter starts for distilled water at an earlier time, the decrease is steeper and has been completed before the crater for 1-Propanol starts collapsing. For both liquids, the same behaviour of the crater walls is noticed, going from straight vertical walls for h_{pool} = 1.5 mm to an increase in diameter one after another for increasing z/h_{pool} for h_{pool} = 6 mm , associated with a clear hemispherical crater (Figure 6).

In Figure 8 we see that the diameter to depth ratios for the two liquids have the same trend. All curves for distilled water lie above the ones for 1-Propanol. The larger the pool depth, the lower this difference between the two liquids. After impact, all craters start with a cylindrical shape (diameter to depth ratio larger than 1), the ratio for distilled water being higher than for 1-Propanol. This is followed by a sharp decrease for distilled water, resulting from a sharper increase in diameter of the crater. As the bottom of the pool is reached, the crater cannot grow further in depth and the diameter to depth ratio increases again and levelling off to a constant value. For a pool depth of 1.5 mm the craters for both liquids stay cylindrical, the craters for distilled water having a larger diameter to depth ratio. As the pool depth is increased, the craters get more hemispherical and for 1-Propanol at h_{pool} = 6 mm the craters are oblate. It is noted that the curves for 1-Propanol (h_{pool} = 3 mm and 6 mm) stay longer at the same level, meaning the craters take longer to collapse.

Conclusions

The time evolution of a crater produced by impact of a drop onto a shallow pool of the same liquid is studied by means of a high-resolution visualisation technique. New information is obtained about the time evolution of the crater depth and crater diameter, as a function of the shallow pool depth, the drop impact velocity and the liquid properties. The results indicate that the depth evolution during crater growth is independent of the drop velocity and liquid properties, until the time instant where the crater has collapsed and starts to retract.

The steepness with which the crater increases in diameter at different depths of the pool decreases as the impact velocity or the pool depth is increased. For low pools the maximum diameter is reached at a later instant and has a higher value due to interaction of the crater with the bottom of the pool. The ratio of the time to reach maximum diameter to the time the crater bottom reverses its direction is about 2 and independent of drop velocity and pool depth. The liquid properties such as the viscosity and surface tension have a clear influence on the process of crater collapse and the accompanying decrease in diameter, as for higher values of these liquid properties this decrease starts earlier and is steeper. For small pool depths the craters stay cylindrical, the craters for distilled water having a larger diameter to depth ratio. As the pool depth is increased, the craters get more hemispherical and for 1-Propanol at a dimensionless pool depth of H^* = 2 the craters are oblate.

Acknowledgements

This work was financed by a grant of the German Research Foundation under No. 520 00558.

References

1. Z. Levin and P.V. Hobbs, Splashing of water drops on solid and wetted surfaces: hydrodynamics and charge separation, *Phil Trans R Soc London A*, vol. 269, pp. 555-585, 1971

2. P. Lenard, Über Wasserfallelektrizität und über die Oberflächenbeschaffenheit der Flüssigkeiten, *Ann Phys*, vol. 47, pp. 463-524, 1915

3. A.L. Yarin, Drop Impact Dynamics: Splashing, Spreading, Receding, Bouncing..., *Annu. Rev. Fluid. Mech.*, vol. 38, pp. 159-192, 2006

4. J. Shin and T.A. McMahon, The tuning of a splash, *Phys. Fluids A*, vol. 2, no. 8, pp. 1312-1317, 1990

5. A.I. Fedorchenko and A.-B. Wang, On some common feature of drop impact on liquid surfaces, *Phys. Fluids*, vol. 16, no. 5, pp. 1349-1365, 2004

6. W.C. Macklin and P.V. Hobbs, Subsurface Phenomena and the Splashing of Drops on Shallow Liquids, *Science*, vol. 166, pp 107-108, 1969